HHS Public Access

Author manuscript

Otolaryngol Head Neck Surg. Author manuscript; available in PMC 2016 February 19.

Published in final edited form as:

Otolaryngol Head Neck Surg. 2015 January ; 152(1): 57–62. doi:10.1177/0194599814552065.

Computer-Aided Designed, 3-Dimensionally Printed Porous Tissue Bioscaffolds For Craniofacial Soft Tissue Reconstruction

David A. Zopf, MD MS[1], **Anna G. Mitsak, PhD**[2], **Colleen L. Flanagan, MSE**[2], **Matthew Wheeler, PhD**[3], **Glenn E. Green, MD**[1], and **Scott J. Hollister, PhD**[2]

[1]Department of Otolaryngology﷿Head and Neck Surgery, ﷿University of Michigan, Ann Arbor, MI, USA

[2]Departments of Biomedical Engineering, Mechanical Engineering, and Surgery, University of Michigan, Ann Arbor, MI, USA

[3]Institute for Genomic Biology & Department of Animal Sciences, University of Illinois, Urbana-Champaign, IL, USA

Abstract

Objectives—To determine the potential of integrated image-based Computer Aided Design (CAD) and 3D printing approach to engineer scaffolds for head and neck cartilaginous reconstruction for auricular and nasal reconstruction.

Study Design—Proof of concept revealing novel methods for bioscaffold production with *in vitro* and *in vivo* animal data.

Setting—Multidisciplinary effort encompassing two academic institutions.

Subjects and Methods—DICOM CT images are segmented and utilized in image-based computer aided design to create porous, anatomic structures. Bioresorbable, polycaprolactone scaffolds with spherical and random porous architecture are produced using a laser-based 3D printing process. Subcutaneous in vivo implantation of auricular and nasal scaffolds was performed in a porcine model. Auricular scaffolds were seeded with chondrogenic growth factors in a hyaluronic acid/collagen hydrogel and cultured *in vitro* over 2 months duration.

Results—Auricular and nasal constructs with several microporous architectures were rapidly manufactured with high fidelity to human patient anatomy. Subcutaneous in vivo implantation of auricular and nasal scaffolds resulted in excellent appearance and complete soft tissue ingrowth. Histologic analysis of in vitro scaffolds demonstrated native appearing cartilaginous growth respecting the boundaries of the scaffold.

Conclusions—Integrated image-based computer-aided design (CAD) and 3D printing processes generated patient-specific nasal and auricular scaffolds that supported cartilage regeneration.

Corresponding author contact information: Scott J. Hollister PhD, Department of Biomedical Engineering, University of Michigan, Lurie Biomedical Engineering Bldg. Rm 2208, 1101 Beal Ave. Ann Arbor, MI 48109-2110, USA. Tel.: + 1 734 647 9962; fax: +1 734 647 0003. scottho@umich.edu (S.J. Hollister).

Accepted for podium presentation at 2013 AAO-HNS Annual Meeting in Vancouver, Ontario

Keywords

auricular reconstruction; microtia; anotia; nasal reconstruction; computer-aided design; computer-aided manufacturing; CAD/CAM; 3 dimensional printing; tissue engineering; craniofacial reconstruction

Introduction

An individual's craniofacial composition contains elaborate soft tissue and cartilaginous structures that impart specific and unique appearance and function. The auricle and nasal framework, when congenitally absent, malformed, oncologically resected, or traumatically distorted are among the most challenging to reconstruct in part due to their complex three dimensional (3D) geometry. At present, auricular and nasal reconstructive techniques most often utilize autologous donor cartilage as foundational support for overlying soft tissue. With advancements in tissue engineering, the technical requirements to recreate these complex cartilaginous structures and limit donor site morbidity may be more effectively met.

Rapid prototyping and three dimensional printing technologies that integrate image-based computer aided design and manufacturing (CAD/CAM) are ideally suited to produce image-based anatomic implants and tissue engineering scaffolds that can reproduce complex craniofacial structures with high fidelity. With tissue engineering advances such as optimization of scaffold pore design, 3D printing of biomaterials, and bioreactor culture capabilities, the geometric and compositional complexity of these structures may be replicable. When seeded with autologous cells, bioresorbable scaffolds may be replaced with native appearing tissue.

This report describes our groups' innovative image-based CAD/CAM and 3D biomaterial printing processes and introduces auricular and nasal scaffolds for soft tissue reconstruction.

Materials and Methods

Scaffold design and manufacturing

Scaffolds were created using image-based hierarchical design methods developed by Hollister and colleages[1–7]. In this approach, hierarchical image designs are created separately for the global anatomic structure, such as the auricle or nose. The design is represented by a density distribution within a voxel format, similar to the way 3D images are represented by density distributions within a voxel dataset. A separate voxel design dataset is created for the anatomic structure, based on the actual patient image data. Heterogeneous structures can be created by designating different voxel densities in different physical locations. Different pore structures are created by generating either a periodic or random distribution of geometric pore structures like spheres and cylinders using density distributions in voxel data structures created by specially written MATLAB™ codes. These codes also map the pore structure over a box that encompasses the final size of the anatomic region. The voxel structure was converted into a triangular surface .STL representation. The final scaffold design is created by mapping the porous architecture STL file into the

appropriate location of the anatomic dataset (also represented as a .STL file after conversion in the commercial software MIMICS™ by Materialise). For the current applications, one porous architecture, either periodic cylinder or random spherical porous, was mapped into the global patient specific anatomic design for the ear or nose using Boolean intersection operations of the custom designed porous architecture .STL file and the anatomic region (auricle or nasal) .STL file using MIMICS to create the final scaffold design.

The final design created by Boolean operation presents a significant manufacturing challenge. Our group[8–11] has developed an approach to laser sinter polycaprolactone (PCL), an FDA approved, resorbable biopolymer. Based on our previous work[9], which established the powder size, bed temperature, and laser sintering power, we used an EOS P100 laser sintering system to fabricate patient specific nose and ear scaffolds. The laser sintering process can fabricate features sizes on the order of 700 microns (0.7mm).

In vitro cartilage growth

Institutional Animal Care Committee protocol approval was obtained. Chondrocytes were isolated from harvested porcine auricular cartilage. Care was taken to isolate cartilage while discarding overlying perichondrium. Minced cartilage fragments were digested with 0.2% type II collagenase (Worthington Biochemical, Lakeview, NJ) for 16 hours in a 37°C, 5% CO2 incubator with agitation. Digest was filtrated through a 70 micron mesh (Becton Dickenson, Franklin Lakes, NJ), the cells were centrifuged to precipitate, counted, and plated. The proliferation medium consisted of Ham's F-12 (Gibco, BRL/Life Technologies, Grand Island, NY), with the addition of 10% fetal bovine serum (FBS, Sigma-Aldrich, St. Louis, MO), 5 mg/ml ascorbic acid, and an antibiotic/antimicotic solution containing 10,000 U/ml penicillin, 10 mg/ml streptomycin, and 25 ug/ml Fungizone.

Chondrocytes were seeded into the auricular PCL scaffolds using a type I collagen gel. The gel solution consisted of type 1 collagen at a concentration of 6 mg/ml in acetic acid (Becton Dickinson, Frankin Lakes, NJ) and hyaluronic acid at a concentration of 3 mg/ml (LifeCore Biomedical, Chaska, MN). Cells were rinsed with Hanks Buffered Saline Solution (HBSS, Gibco, BRL/Life Technologies, Grand Island, NY), trypsinized (0.25% trypsin, Gibco), aliquoted into 15 ml conical tubes and placed on ice. Prior to seeding, the PCL scaffolds were placed in custom-designed sylgard (Dow Corning, Midland, MI) molds to prevent leakage of the cell-collagen solution prior to gelation. After resuspending the cells in the collagen I gel solution, sodium bicarbonate was added, the cell suspension was carefully pipetted into the PCL scaffolds and the constructs were placed in an incubator (37°C, 5% CO_2) for 30 minutes for gelation to occur. The chondrocyte seeding density was 25×10^6 cells/cm3. Seeded constructs were cultured in sterile, dynamic conditions with incubation at 37°C, 5% CO_2. The culture medium consisted of serum free F12 (Gibco), with the addition of 5 ng/ml TGF-β 2 (Pepro Tech, Rocky Hill, NJ), ITS+premix (Becon Dickinson), 110mm pyruvate (Gibco), 10um dexamethasone (Sigma), and 5 ug/ml ascorbic acid.

After 8 weeks, ear constructs were histologically analyzed. The specimens were fixed with 10% phosphate buffered formalin for 24 h, and then embedded in paraffin and sectioned using standard histochemical techniques. Serial slide sections were stained with hematoxylin and eosin or Safranin O.

In vivo scaffold implantation

Adult Yorkshire pigs were used to demonstrate scaffold appearance with soft tissue coverage. General anesthetic was administered. A postauricular incision was performed with development of supraperichondrial soft tissue flaps for placement of auricular and nasal scaffolds. 3-0 vicryl suture was used to secure the overlying soft tissue to the scaffolds. Layered skin closure was performed with 3-0 vicryl and a 4-0 monocryl subcuticular closure.

Results

Using these techniques nasal and auricular scaffolds were produced with high anatomic fidelity at a rate of approximately 50 scaffolds in 4-5 hours. A vast array of porous architectures are available for incorporation into the anatomic scaffold design. A representative spherical pore auricular scaffold and random pore nasal scaffold are depicted in Figures 1 and 2 respectively.

The porosity of the 3 dimensionally printed scaffolds allow for infusion of hydrogels. For our purposes, type I collagen, hyaluronic acid, and TGF β-2 impregnated hydrogel cell carriers were utilized. In vitro culture of porcine auricular chondrocytes in these scaffolds resulted in growth and maintenance of cartilage-like tissue after 8 weeks, as evidenced by representative histological staining shown in Figure 3.

Surgical implantation of scaffolds was performed with ease and scaffold porosity allowed for versatility and ease of suture placement. The PCL material maintained excellent foundational support and appearance when implanted in subcutaneous tissue.

PCL scaffolds all demonstrated histologically native appearing cartilage growth. At two months duration in vitro, scaffolds had not reached complete confluent cartilage coverage.

Discussion

Auricular reconstruction, performed for an unsalvageable auricle in the setting of trauma, oncologic resection, microtia, or anotia, is one of the most technically challenging surgical procedures in reconstructive surgery[12]. A limited number of surgeons have mastered the art of using autogenous rib cartilage[13,14], the current gold standard, to carve a auricular cartilage framework. Costal cartilage auricular reconstruction is a highly complex procedure requiring multiple surgeries – each with accompanying anesthetic exposures and risks. Outcomes and complication rates are highly dependent on surgical experience.

An alternative option for autologous rib auricular reconstruction is prefabricated, synthetic MedPor, or porous high-density polyethylene (PHDPE)[15]. Benefits of this technique include avoiding donor site morbidity from rib harvest and lower variability with framework appearance, bypassing the technically demanding framework carving. Frameworks are not available for patient specific anatomy. MedPor is FDA-approved, though being a rigid, synthetic material has a greater incidence of framework extrusion and soft tissue necrosis than autogeneous cartilage reconstruction[16].

Similarly, total and partial nasal reconstruction can be a highly complex and laborious challenge to the most experienced reconstructive surgeon. Addressing patients requiring total nasal reconstruction often involves utilization of multiple autogenous tissue donor components. Split calvarial bone, auricular conchal cartilage, and rib have been employed for nasal reconstruction. Pedicled paramedian forehead, interpolated cheek, nasal septal hinge flaps, and free soft tissue often harvested from the radial forearm have been used to reproduce an overlying soft tissue envelope[17–19]. Sultan and Byrne have previously described the use of rapid prototyping to create a translucent intraoperative template to guide total nasal reconstruction[20].

Advances in tissue engineering have made the prospect for a fabricated cartilaginous framework a realistic potential. A recent review by Nayyer et al, details numerous studies examining a variety of scaffolds, cell sources, growth factors and cell culture methods[21]. Several studies have demonstrated that auricular chondrocytes, as opposed to other cartilage sources, or mesenchymal stems cells with pro-chondrogenic growth factors are able to develop tissue-engineered cartilage that is histologically and mechanically similar to native ear cartilage[22–24]. As advancements in auricular tissue engineering have been made, new challenges have surfaced.

One obstacle to auricular tissue engineering based auricle reconstruction is building and maintaining an auricle cartilage framework that maintains anatomical landmarks preserves size and shape. Shieh et al produced scaffolds by packing a bioresorbable polymer into a negative clay mold of the auricle[25]. CT-based- fused deposition modeling has been employed to form polyurethane frameworks, which were then implanted *in vivo* but described with minimal detail with regards to outcomes at 12 weeks after implantation other than a “fair result” with gross morphology remaining “well” [26]. Liu et al describes CAD use for producing a negative mold and evaluating the resulting framework shape[27].

This is the first report to our knowledge in peer-reviewed literature describing patient specific, image-based design and laser sintering 3D printing to produce a bioresorbable PCL scaffold with defined porous architecture for auricular and nasal reconstruction. Furthermore, it is the first description to our knowledge of the use of 3D printing to produce bioresorbable nasal scaffolds with incorporated pore architecture. Our process is able to rapidly produce high fidelity anatomic scaffolds while also allowing meticulous control of pore microarchitecture.

The patient specific image-based design incorporates DICOM data as a mapping for designed porous architecture. The porous architecture is generated using MATLAB or similar numerical software programs to delineate porous structures in a 3D regular space (e.g. a cylinder or cube). This 3D architecture is intersected with a density distribution in 3D space from patient image data to create a patient specific scaffold construct with the desired designed pore architecture. The resulting construct is then converted into STL format for 3D printing. Our 3D printing process utilized a laser sintering process. In essence, an individuals unique radiologic imaging DICOM data is used to render a CAD model. Architectural details are added to the CAD model which then serves to dictate the selective fusion of PCL powder layer by layer and creates scaffolds from the bottom up. The ability to

control pore architecture is unique to our laser sintering process and was recently shown by our group to have chondrogenic potential[28]. Combining precise pore architecture for chondrogenicity with previously described prochondrogenic growth factors may allow for rapid production of patient specific ear constructs with anatomic detail, dimension preservation, and patient satisfaction.

Animal studies are currently underway to delineate whether imparting scaffolds with defined pore architecture using a material with a longer resorption profile, such as PCL, will prevent framework contraction. We are additionally pursuing experiments comparing the effect of particular porous architectures on outcomes such as duration to confluent cartilaginous framework coverage and biomechanical properties. Our report does not include biochemical and biomechanical profiles comparing our tissue engineered constructs to native cartilage, though analysis is planned in combination with our long term *in vivo* data.

Conclusions

A novel image-based CAD/CAM 3D printing process in the production of bioresorbable PCL scaffolds with defined porous architecture for cartilaginous frameworks is introduced. Our technique utilizes 3D printing for auricle and nose scaffold production and control of pore architecture, which may provide a tool to advance tissue engineering in this area. Further analysis is needed to ultimately define performance and potential improvements over current surgical and tissue engineering techniques.

References

1. Hollister SJ, Levy RA, Chu TMJ, et al. An Image Based Approach to Design and Manufacture Craniofacial Scaffolds. Int J Oral﷒Maxillofac Surg. 2000; 29:67–71. [PubMed: 10691148]
2. Hollister SJ, Maddox RD, Taboas JM, et al. Optimal Design and Fabrication of Scaffolds to Mimic Tissue Properties and Satisfy Biological Constraints. Biomaterials. 2002; 23:4095–4103. [PubMed: 12182311]
3. Lin CY, Kikuchi N, Hollister SJ. A novel method for biomaterial scaffold internal architecture design to match bone elastic properties with desired porosity. J. Biomechanics. 2004; 37:623–636.
4. Hollister SJ, Lin CY, Saito E, et al. Engineering craniofacial scaffolds. Orthod Craniofac Res. 2002; 8:162–173. [PubMed: 16022718]
5. Hollister SJ. Porous scaffold design for tissue engineering. Nat Mater. 2005; 4:518–524. [PubMed: 16003400]
6. Hollister SJ, Lin CY. Computational Design of Tissue Engineering Scaffolds. Computer Methods in App. Mech. and Eng. 2005; 196:2991–2998.
7. Kang H, Lin CY, Hollister SJ. Topology optimization of three dimensional tissue engineering scaffold architectures for prescribed bulk modulus and diffusivity. Struct Multidiscip O. 2010; 42:633–644.
8. Williams JM, Adewunmi A, Schek RM, et al. Bone tissue engineering using polycaprolactone scaffolds fabricated via selective laser sintering. Biomaterials. 2005; 26:4817–4827. [PubMed: 15763261]
9. Partee B, Hollister SJ, Das S. Selective laser sintering process optimization for layered manufacturing of CAPA 6501 Polycaprolactone Bone Tissue Engineering Scaffolds. J Manuf Sci E. 2006; 128:531–540.
10. Smith M, Flanagan CL, Kemppainen JM, et al. Computed tomography-based tissue engineered scaffolds in craniomaxillofacial surgery. Int. J. Med Robot Comp. 2007; 3:207–216.

11. Mitsak AG, Kemppainen JM, Harris M, et al. Effect of polycaprolactone permeability on bone regeneration in vivo. Tissue Eng. 2011; 17:1831–1839.
12. Bichara DA, O'Sullivan NA, Pomerantseva I, et al. The tissue-engineered auricle: Past, present, and future. Tissue Eng Part B Rev. 2012; 18(1):51–61. [PubMed: 21827281]
13. Brent B. The correction of microtia with autogenous cartilage grafts, the classic deformity. Plast Reconstr Surg. 1980; 66(1):1–12. [PubMed: 7394028]
14. Nagata S. A new method of total reconstruction of the auricle for microtia. Plast Reconstr Surg. 1993; 92(2):187–201. [PubMed: 8337267]
15. Romo T 3rd, Presti PM, Yalamanchili HR. Medpor alternative for microtia repair. Facial Plast Surg Clin North Am. 2006; 14(2):129–36. [PubMed: 16750770]
16. Zhao YY, Zhuang HX, Jiang HY, et al. Clinical application of three methods for total ear reconstruction. Zhonghua Zheng Xing Wai Ke Za Zhi. 2008; 24(4):287–290. [PubMed: 18950023]
17. Baker, SR. Principles of Nasal Reconstruction. Springer; 2011.
18. Winslow CP, Cook TA, Burke A, et al. Total nasal reconstruction: Utility of the free radial forearm fascial flap. Arch Facial Plast Surg. 2003; 5(2):159–163. [PubMed: 12633204]
19. Henry EL, Hart RD, Mark Taylor S, et al. Total nasal reconstruction: Use of a radial forearm free flap, titanium mesh, and a paramedian forehead flap. J Otolaryngol Head Neck Surg. 2010; 39(6): 697–702. [PubMed: 21144366]
20. Sultan B, Byrne PJ. Custom-Made, 3D, Intraoperative Surgical Guides for Nasal Reconstruction. Facial Plast Surg Clin North Am. 2011; 19:4, 647–653.
21. Nayyer, Patel KH.; Esmaieli, A. Tissue Engineering: Revolution and Challenge in Auricular Cartilage Reconstruction. Plast Reconstr Surg. 2013; 129:5, 1123–1137.
22. Isogai N, Kusuhara H, Ikada Y, et al. Comparison of different chondrocytes for use in tissue engineering of cartilage model structures. Tissue Eng. 2006; 12:4, 691–703.
23. van Osch GJ, van der Veen SW, Verwoerd-Verhoef HL. In vitro redifferentiation of culture-expanded rabbit and human auricular chondrocytes for cartilage reconstruction. Plast Reconstr Surg. 2001; 107(2):433–440. [PubMed: 11214059]
24. Vacanti CA, Cima LG, Ratkowski D, et al. Tissue engineered growth of new cartilage in the shape of a human ear using synthetic-polymers seeded with chondrocytes. 1992. Tissue-Inducing Biomaterials, Materials Research Soc. Symposium Proceedings. 252:367–374.
25. Shieh SJ, Terada S, Vacanti JP. Tissue engineering auricular reconstruction: In vitro and in vivo studies. Biomaterials. 2004; 25(9):1545–1557. [PubMed: 14697857]
26. Zeng W, Lin F, Shi T, et al. Fused deposition modelling of an auricle framework for microtia reconstruction based on CT images. Rapid Prototyping J. 2008; 14(5):280–284.
27. Liu Y, Zhang L, Zhou G, et al. In vitro engineering of human ear-shaped cartilage assisted with CAD/CAM technology. Biomaterials. 2010; 31(8):2176–2183. [PubMed: 20022366]
28. Kemppainen JM, Hollister SJ. Differential effects of designed scaffold permeability on chondrogenesis by chondrocytes and bone marrow stromal cells. Biomaterials. 2010; 31(2):279–287. [PubMed: 19818489]

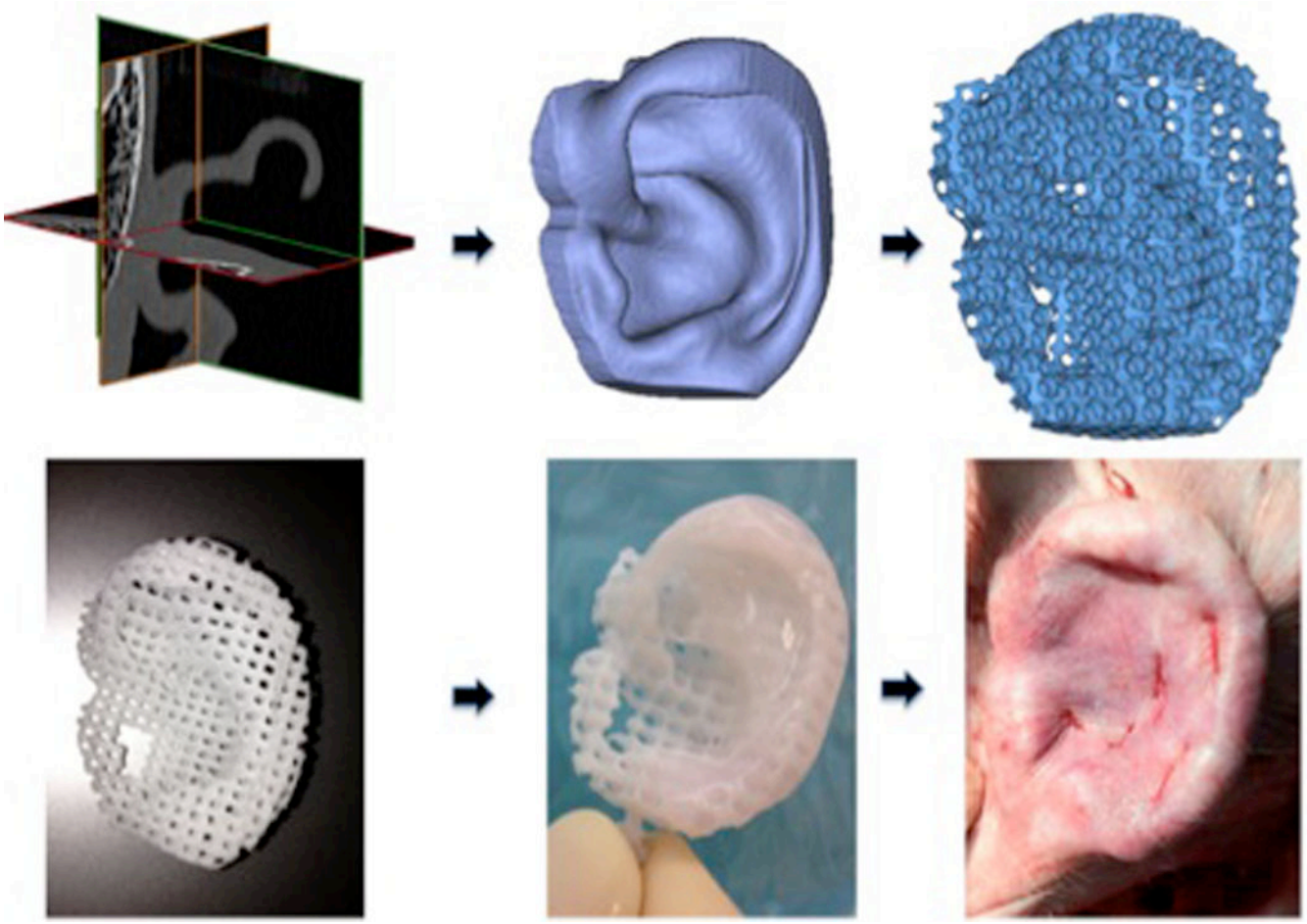

Figure 1.
Auricular CAD/CAM 3D printed polycaprolactone scaffold. Patient CT (upper left), CAD rendering (upper middle), pore incorporation (upper right), 3D-printed ear (lower left), with hydrogel (lower middle), in vivo implantation (lower right).

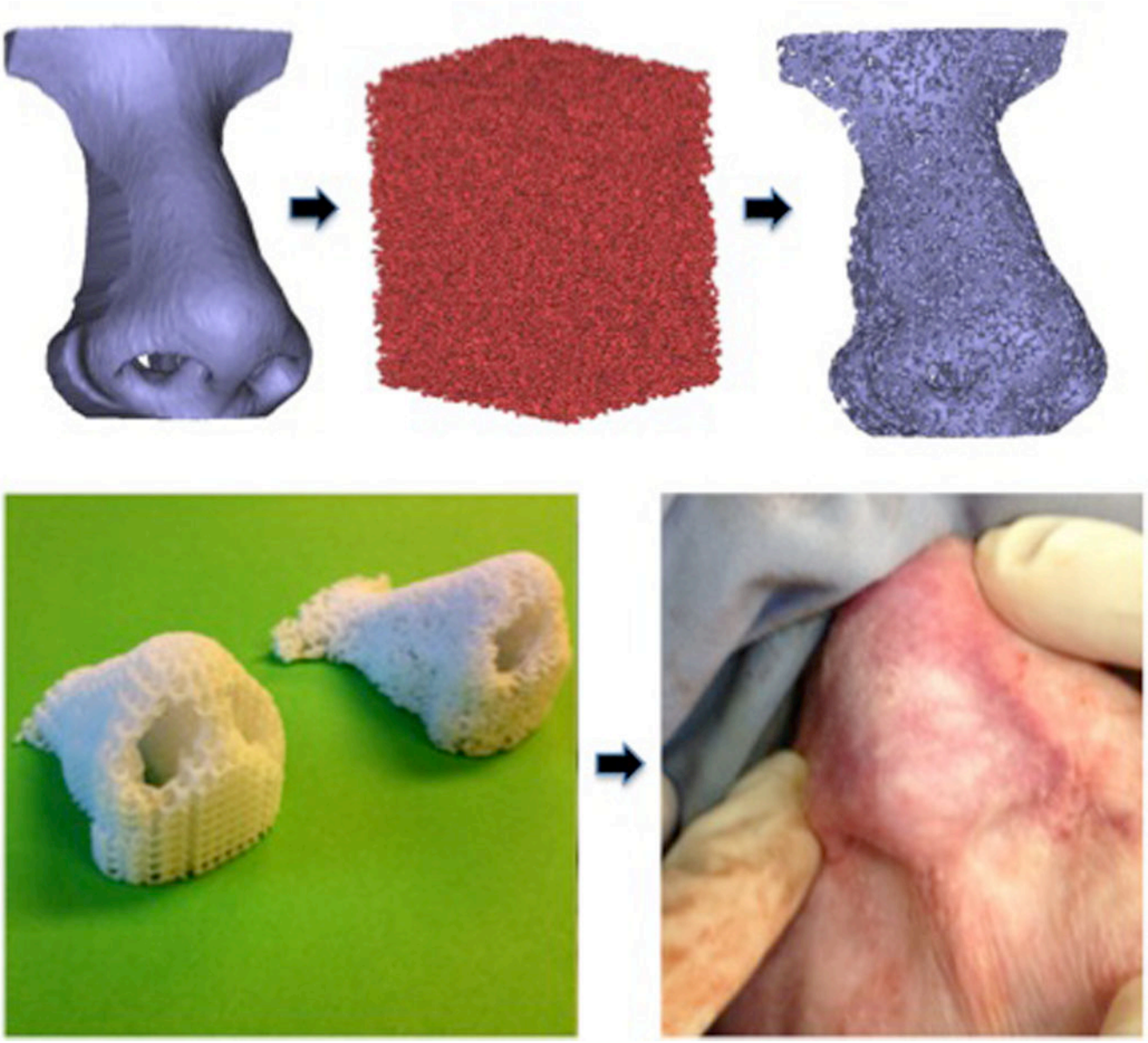

Figure 2.
Nasal CAD/CAM 3D printed polycaprolactone scaffolds, left, spherical pore design, right, random pore design (left), and after immediate porcine post-auricular subcutaneous implantation (right).

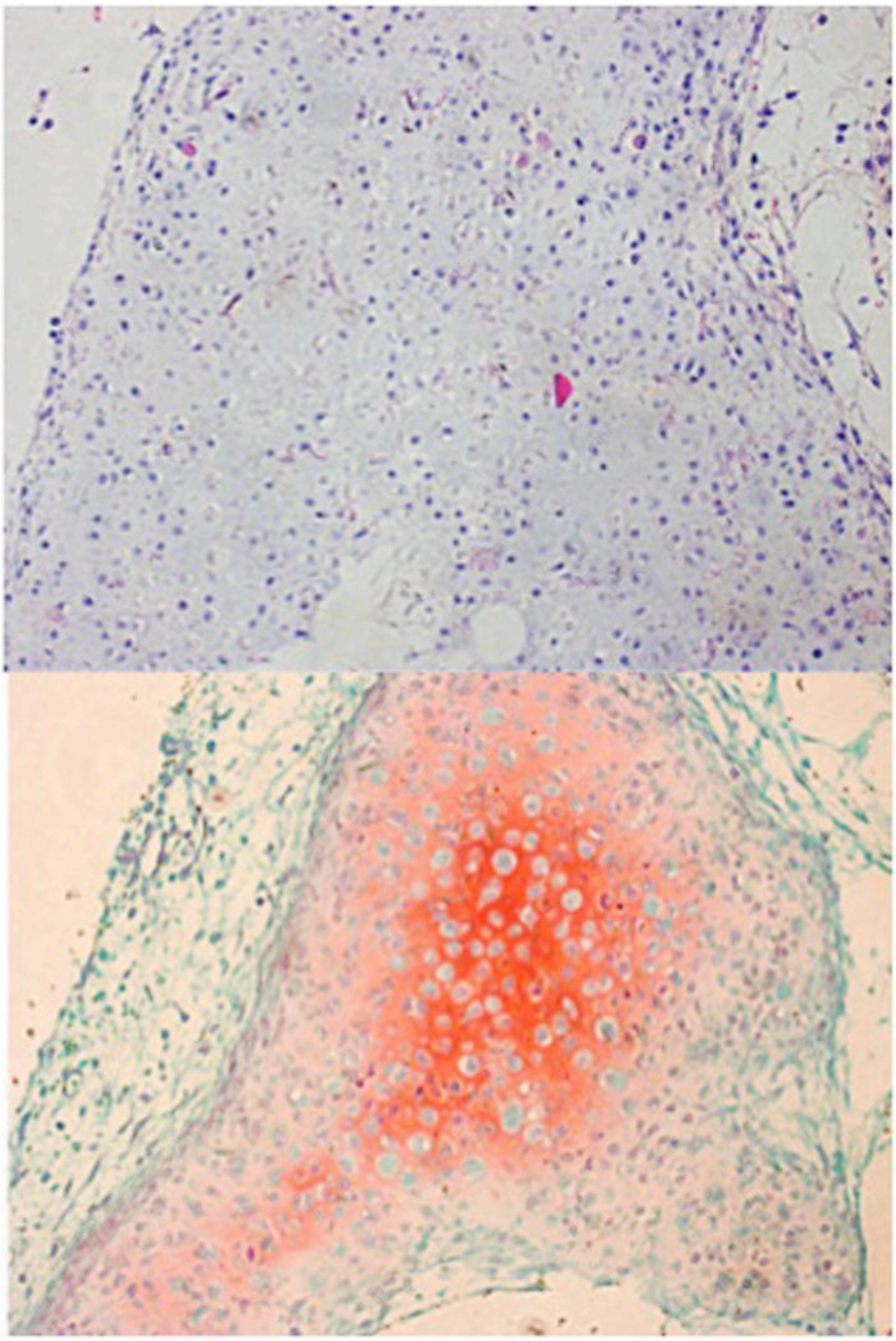

Figure 3.
In vitro, primary porcine chondrocyte growth on PCL scaffolds (H&E, top; Safranin O, middle. 20X); mouse epiphyseal plate cartilage, positive comparison, brackets encompassing cartilaginous component (Safranin O, 20X, bottom).